Proceedings of 2004 IEEE/RSJ International Conference on
Intelligent Robots and Systems
September 28 - October 2, 2004, Sendai, Japan

Stabilization of a mini-rotorcraft having four rotors

P. Castillo, R. Lozano
Heudiasyc - UTC UMR CNRS 6599
Compiègne, France.
Email: castillo@hds.utc.fr, rlozano@hds.utc.fr

A. Dzul
Instituto Tecnológico de la Laguna
Torreón, Coahuila, México
Email: dzul@itlalaguna.edu.mx

Abstract— **In this paper we present a controller design and implementation on a mini-rotorcraft having four rotors. A Lagrangien model of the helicopter was used for the controller synthesis. The proposed controller is based on Lyapunov analysis. Experimental results show that the controller is able to perform autonomously the tasks of taking-off, hovering and landing.**

I. INTRODUCTION

Flight control problems for small unmanned helicopters and some special airplanes has attracted the attention of control researches in the last decade. The classical control strategies for helicopters basically assumed a linear model obtained for a particular operating point. The use of modern nonlinear control theory should improve the performance of the controller and allow the tracking of agressive trajectories.

In this paper we obtain a nonlinear model for a four-rotor mini-rotorcraft and propose a nonlinear control strategy based on Lyapunov analysis. The problem is closely related to the problem of controlling a PVTOL *i.e.* Planar Vertical Take-off and Landing aircraft. Generally, the control strategies are based on simplified models which have both a minimum number of states and a minimum number of inputs. These reduced models should retain the main features that must be considered when designing control laws for real aerial vehicles.

The classical helicopter is one of the most complex flying objects. The classical helicopter is basically equipped of a main rotor and a tail rotor.

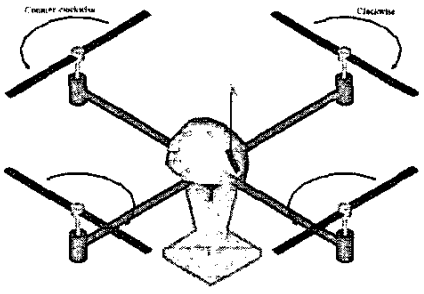

Fig. 1. Blades rotation direction in the four-rotor rotorcraft.

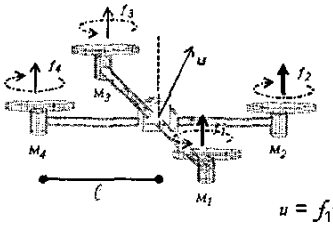

$$u = f_1+f_2+f_3+f_4$$
$$f_i = k_i w_i^2 \quad i = 1, \ldots, 4$$

Fig. 2. The throttle control input.

However other type of helicopters exist including the twin rotor or tandem helicopter and the co-axial rotor helicopter. We are particularly interested in controlling a mini-rotorcraft having four rotors (see Fig. 1).

A. CHARACTERISTICS OF THE FOUR-ROTOR ROTORCRAFT

In this type of helicopters the front and the rear motors rotate counter-clockwise while the other two rotate clockwise (see Fig. 1), gyroscopic effects and aerodynamic torques tend to cancel in trimmed flight.

The four-rotor rotorcraft does not have a swashplate as standard helicopters. In fact it does not need any servomechanism. The main thrust is the sum of the thrusts of each motor (see Fig. 2). Pitch movement is obtained by increasing (reducing) the speed of the rear motor while reducing (increasing) the speed of the front motor. The roll movement is obtained similarly using the lateral motors (see Fig. 3).

The yaw movement is obtained by increasing (decreasing) the speed of the front and rear motors while decreasing (increasing) the speed of the lateral motors. This should be done while keeping the total thrust constant (see Fig. 3).

In view of its configuration, the four-rotor rotorcraft in figure 1 has some similarities with the PVTOL (Planar Vertical Take Off and Landing aircraft) problem. Indeed, if the roll and yaw angles are set to zero, the four-rotor rotorcraft reduces to a PVTOL (see Fig. 3a). In a way the four-rotor rotorcraft can be seen as two PVTOL connected such that their axes are orthogonal (see Fig. 3a and 3b).

0-7803-8463-6/04/$20.00 ©2004 IEEE

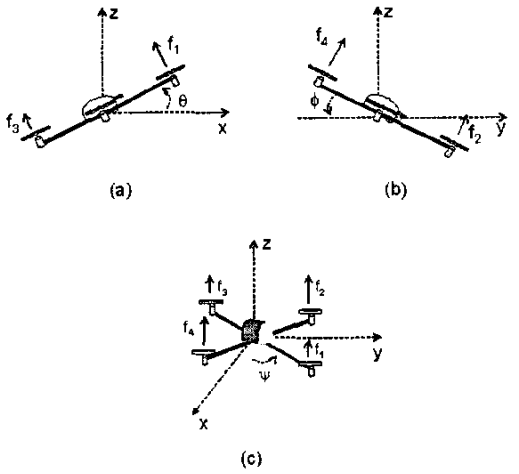

Fig. 3. (a) Pitch. (b) roll and (c) yaw control inputs.

This article begins with a introduction that describes the main characteristics of the mini-rotorcraft having four rotors. After, we present the dynamical model obtained via a Lagrange approach. A control strategy is proposed having in mind that the four rotor rotorcraft can be seen as the interconnection of two PVTOL.

The control algorithm is based on saturation control strategy. We then prove global stability of the proposed controller. Furthermore the controller has been implemented on a PC and real time experiments have shown that the proposed control strategy performs well in practice. Finally, we discuss some conclusions.

II. Dynamical Model

In this section we will describe the dynamical model we have used for the four-rotor mini-rotorcraft. This model is basically obtained representing the mini-rotorcraft as a solid body evolving in 3D and subject to one force and 3 moments [10]. The four electric motors' dynamics is relatively fast and therefore it will be neglected as well as the flexibility of the blades. The generalized coordinates of the rotorcraft are

$$q = (x, y, z, \psi, \theta, \phi) \in R^6$$

where $(x, y, z) = \xi \in \Re^3$ denote the position of the center of mass of the four-rotor rotorcraft relative to the frame $\mathcal{I}$ and $(\psi, \theta, \phi) = \eta \in \Re^3$ are the three Euler angles (yaw, pitch and roll) [8], [9] and represent the orientation of the rotorcraft (see figure 4).

The Lagrangian of the rotorcraft is

$$L(q, \dot{q}) = T_{trans} + T_{rot} - U$$

where $T_{trans} = \frac{m}{2}\dot{\xi}^T\dot{\xi}$ is the translational kinetic energy, $T_{rot} = \frac{1}{2}\dot{\eta}^T\mathbb{J}\dot{\eta}$ is the rotational kinetic energy, $U = mgz$ is the potential energy of the rotorcraft, z is the rotorcraft altitude, m denotes the mass of the rotorcraft, the matrix $\mathbb{J}$ represents the inertia matrix and g is the gravity.

The model of the full rotorcraft dynamics is obtained from the Euler-Lagrange Equations with external generalized forces

$$\frac{d}{dt}\frac{\partial \mathcal{L}}{\partial \dot{q}} - \frac{\partial \mathcal{L}}{\partial q} = (F_\xi, \tau)$$

where $F_\xi = R\widehat{F}$ is the translational force applied to the rotorcraft due to the throttle control input, $\tau \in \Re^3$ represents the pitch, roll and yaw moments, and R denotes the rotational matrix $R(\psi, \theta, \phi) \in SO(3)$ representing the orientation of the rotorcraft relative to a fixed inertial frame $(\mathcal{I})$ (see figure 5). From figures (2) and (4) we have that $\widehat{F}$ is a vector given by

$$\widehat{F} = \begin{pmatrix} 0 \\ 0 \\ u \end{pmatrix} \tag{1}$$

where u is the collective control input expressed as

$$u = \sum_{i=1}^{4} f_i$$

and f_i is the force produced by motor M_i, $i = 1, .., 4$ as shown in (2). Typically $f_i = k_i\omega_i^2$ where k_i is a constant and ω_i is the angular velocity of the *i-th* motor. The generalized torques are thus

$$\tau = \begin{pmatrix} \tau_\psi \\ \tau_\theta \\ \tau_\phi \end{pmatrix} \triangleq \begin{pmatrix} \sum_{i=1}^{4} \tau_{M_i} \\ (f_2 - f_4)\ell \\ (f_3 - f_1)\ell \end{pmatrix} \tag{2}$$

where ℓ is the distance between the motors and the center of gravity and τ_{M_i} is the moment produced by motor M_i, $i = 1, .., 4$. around the center of gravity of the aircraft.

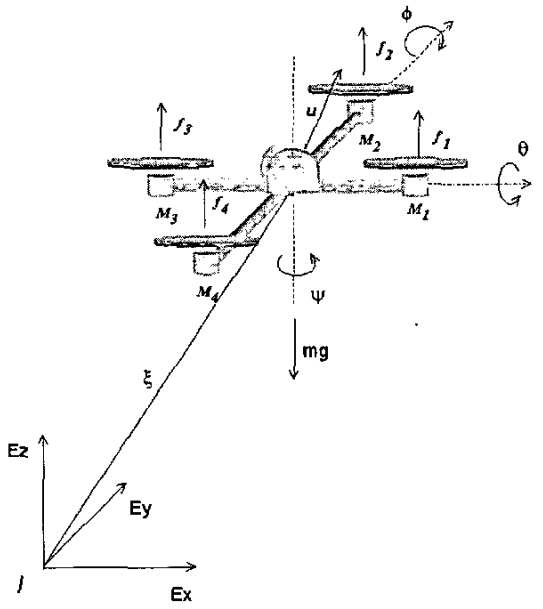

Fig. 4. Schema of the four-rotor rotorcraft.

Since the Lagrangian contains no cross terms in the kinetic energy involving $\dot{\xi}$ and $\dot{\eta}$, the Euler Lagrange equations can be partitioned into two parts. One part for the dynamics of the ξ coordinates and the other part for the η coordinates. One obtains

$$m\ddot{x} = -u\sin\theta \quad (3)$$
$$m\ddot{y} = u\cos\theta sin\phi \quad (4)$$
$$m\ddot{z} = u\cos\theta\cos\phi - mg \quad (5)$$
$$\ddot{\psi} = \tilde{\tau}_\psi \quad (6)$$
$$\ddot{\theta} = \tilde{\tau}_\theta \quad (7)$$
$$\ddot{\phi} = \tilde{\tau}_\phi \quad (8)$$

where x and y are the coordinates in the horizontal plane, and z is the vertical position (see figure 4). ψ is the yaw angle around the z-axis, θ is the pitch angle around the (new) y-axis, and ϕ is the roll angle around the (new) x-axis. We use the notation c_θ for $\cos\theta$ and s_θ for $\sin\theta$. u is the thrust directed out the bottom of the aircraft and $\tilde{\tau}_\psi$, $\tilde{\tau}_\theta$ and $\tilde{\tau}_\phi$ are the moments (yawing moment, pitching moment and rolling moment), which are related to the generalized torques $\tau_\psi, \tau_\theta, \tau_\phi$ as follows:

$$\tilde{\tau} = \begin{pmatrix} \tilde{\tau}_\psi \\ \tilde{\tau}_\theta \\ \tilde{\tau}_\phi \end{pmatrix} = \mathbb{J}^{-1}(\tau - C(\eta,\dot{\eta})\dot{\eta})$$

where $C(\eta,\dot{\eta})$ is the Coriolis matrix.

III. Control Strategy

In this section we will develop a control strategy for stabilizing the rotorcraft at hover.

The controller synthesis procedure regulates each of the states variables in a sequence using a priority rule as follows:

We first design a control to stabilize the yaw angular displacement. We then control the roll angle ϕ and the y-displacement using a controller designed for a PVTOL.

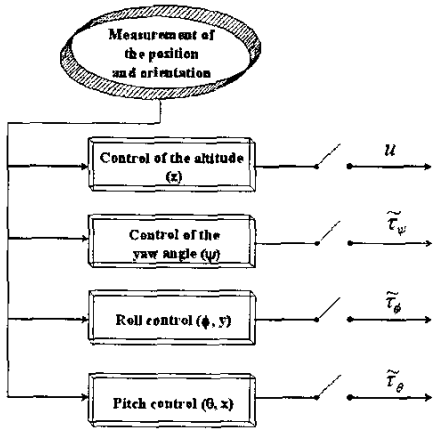

Fig. 5. Manual/Automatique switch diagram.

Phase	Name	Description
1	Control Altitude	u is used to make the altitude reach a desired value
2	Yaw control	$\tilde{\tau}_\psi$ is used to set the yaw displacement to zero
3	Roll Control	$\tilde{\tau}_\phi$ is used to control the roll ϕ and the horizontal movement in the y-axis
4	Pitch Control	$\tilde{\tau}_\theta$ is used to control the pitch θ and the horizontal movement in the x-axis

TABLE I
Control Strategy Sequence

Finally the pitch angle θ and the x-displacement are controlled using again a strategy designed for the PVTOL.

The proposed control strategy is relatively simple. This property is important when performing real-time applications. Furthermore, the four control inputs can independently operate in either manual or automatic mode . For flight safety reasons this feature is particularly important when implementing the control strategy.

Roughly speaking each of the control inputs can be used to control one or two degrees of freedom as follows: The control input u is essentially used to make the altitude reach a desired value. The control input $\tilde{\tau}_\psi$ is used to set the yaw displacement to zero. $\tilde{\tau}_\theta$ is used to control the pitch angle and the horizontal movement in the x - axis. Similarly $\tilde{\tau}_\phi$ is used to control the roll angle and the horizontal displacement in the y-axis.

A. Control of the altitude and yaw displacement

The control of the altitude is obtained by using the following control input.

$$u = -(r_1 + mg)\frac{1}{c_\theta c_\phi} \quad (9)$$

where

$$r_1 = -a_{z_1}\dot{z} - a_{z_2}(z - z_d) \quad (10)$$

where a_{z_1}, a_{z_2} are positive constants and z_d is the desired altitude. The yaw angular position can be controlled by applying

$$\tilde{\tau}_\psi = -a_{\psi_1}\dot{\psi} - a_{\psi_2}(\psi - \psi_d) \quad (11)$$

Indeed, introducing (9)-(11) into (3)-(6) and provided $c_\theta c_\phi \neq 0$, we obtain

$$m\ddot{x} = -(r_1 + mg)\frac{\tan\theta}{\cos\phi} \quad (12)$$
$$m\ddot{y} = (r_1 + mg)\tan\phi \quad (13)$$
$$\ddot{z} = \frac{1}{m}(-a_{z_1}\dot{z} - a_{z_2}(z - z_d)) \quad (14)$$
$$\ddot{\psi} = -a_{\psi_1}\dot{\psi} - a_{\psi_2}(\psi - \psi_d) \quad (15)$$

The control parameters a_{ψ_1}, a_{ψ_2}, a_{z_1}, a_{z_2} should be carefully chosen to ensure a stable well-damped response of the rotorcraft.

From equation (14), (10) and (15) it follows that $\psi \rightarrow \psi_d$ and $z \rightarrow z_d$.

B. Control of the roll angle and the horizontal movement in the y-axis

We will now find the input $\tilde{\tau}_\phi$ to control $\dot{\phi}, \phi, \dot{y}$ and y. The control algorithm will be obtained step by step. The final expression for $\tilde{\tau}_\phi$ will be given at the end of this section (see 46). Roughly speaking, for ϕ close to zero, the (x, ϕ) subsystem is represented by four integrators in cascade.

We will first consider the subsystem given by (8) and (13). For simplicity we chose $\psi_d \equiv 0$. Therefore, from (15) it follows that $\psi \rightarrow 0$. Note also that from (10) and (14) that $r_1 \rightarrow 0$. For a time T large enough, r_1 and ψ are arbitrarily small.

To simply further the analysis we will chose the amplitude of the saturation function in the nested saturation control law in such a way that after a some finite time, $|\phi| < 1$. Therefore, the difference $\tan(\phi) - \phi$ is also small. Thus, the subsystem (8), (13) reduces to

$$\ddot{y} = g\phi \tag{16}$$
$$\ddot{\phi} = \tilde{\tau}_\phi \tag{17}$$

which represents four integrators in cascade.

1) Boundedness of $\dot{\phi}$: In order to establish a bound for $\dot{\phi}$ let $\tilde{\tau}_\phi$ be

$$\tilde{\tau}_\phi = -\sigma_{\phi_1}(\dot{\phi} + \sigma_{\phi_2}(\zeta_{\phi_1})) \tag{18}$$

where $\sigma_i(s)$ is a saturation function such that $\mid \sigma_i(s) \mid \leq M_i$ for $i = 0, 1, ...$ and ζ_{ϕ_1} will be defined later to ensure global stability.

We propose the following Lyapunov function

$$V = \frac{1}{2}\dot{\phi}^2 \tag{19}$$

Differentiating V, we obtain

$$\dot{V} = \dot{\phi}\ddot{\phi} \tag{20}$$

and from the equation (17) and (18) we have

$$\dot{V} = -\dot{\phi}\sigma_{\phi_1}(\dot{\phi} + \sigma_{\phi_2}(\zeta_{\phi 1})) \tag{21}$$

Note that if $\mid \dot{\phi} \mid > M_{\phi_2}$ then $\dot{V} < 0$, i.e. $\exists T_1$ such that $\mid \dot{\phi} \mid \leq M_{\phi_2}$ for $t > T_1$.

We define

$$\nu_1 \equiv \phi + \dot{\phi} \tag{22}$$

Differentiating (22)

$$\dot{\nu}_1 = \dot{\phi} + \ddot{\phi} \tag{23}$$
$$= \dot{\phi} - \sigma_{\phi_1}(\dot{\phi} + \sigma_{\phi_2}(\zeta_{\phi_1})) \tag{24}$$

Let us choose

$$M_{\phi_1} \geq 2M_{\phi_2} \tag{25}$$

From the definition of $\sigma(s)$ we can see that $\mid \sigma_i(s) \mid \leq M_i$. This implies that in a finite time, $\exists T_1$ such that $\mid \dot{\phi} \mid \leq M_{\phi_2}$ for t$\geq T_1$. Therefore, for $t \geq T_1$, $\mid \dot{\phi} + \sigma_{\phi_2}(\zeta_{\phi_1}) \mid \leq 2M_{\phi_2}$. It then follows that, $\forall t \geq T_1$

$$\sigma_{\phi_1}(\dot{\phi} + \sigma_{\phi_2}(\zeta_{\phi_1})) = \dot{\phi} + \sigma_{\phi_2}(\zeta_{\phi_1}) \tag{26}$$

Using (24) and (26), we get

$$\dot{\nu}_1 = -\sigma_{\phi_2}(\zeta_{\phi_1}) \tag{27}$$

Then, from (7), (18) and (26) we obtain for $t \geq T_1$

$$\ddot{\phi} = -\dot{\phi} - \sigma_{\phi_2}(\zeta_{\phi_1}) \tag{28}$$

2) Boundedness of ϕ: To establish a bound for ϕ, define ζ_{ϕ_1} as

$$\zeta_{\phi_1} \equiv \nu_1 + \sigma_{\phi_3}(\zeta_{\phi_2}) \tag{29}$$

Introducing the above in (27) it follows

$$\dot{\nu}_1 = -\sigma_{\phi_2}(\nu_1 + \sigma_{\phi_3}(\zeta_{\phi_2})) \tag{30}$$

The upper bounds are assumed to satisfy

$$M_{\phi_2} \geq 2M_{\phi_3} \tag{31}$$

This implies that $\exists T_2$ such that $\mid \nu_1 \mid \leq M_{\phi_3}$ for t$\geq T_2$. From equation (22) we can see that $\forall t \geq T_2$, $\mid \phi \mid \leq M_{\phi_3}$. M_{ϕ_3} should be chosen small enough such that $\tan(\phi) \approx \phi$.

From (30) and (31), we have that for $t \geq T_2$, $\mid \nu_1 + \sigma_{\phi_3}(\zeta_{\phi_2}) \mid \leq 2M_{\phi_3}$. It then follows that, $\forall t \geq T_2$

$$\sigma_{\phi_2}(\nu_1 + \sigma_{\phi_3}(\zeta_{\phi_2})) = \nu_1 + \sigma_{\phi_3}(\zeta_{\phi_2}) \tag{32}$$

Then, in view of the above, (30) reduces to

$$\dot{\nu}_1 = -\nu_1 - \sigma_{\phi_3}(\zeta_{\phi_2})$$

for $t \geq T_2$.

3) Boundedness of $\dot{y}$: To establish a bound for $\dot{y}$, let us introduce the following function

$$\nu_2 \equiv \nu_1 + \phi + \frac{\dot{y}}{g} \tag{33}$$

then

$$\dot{\nu}_2 = \dot{\nu}_1 + \dot{\phi} + \frac{\ddot{y}}{g} \tag{34}$$

Using (16), (22), (30) and (32) into (34), we obtain

$$\dot{\nu}_2 = -\sigma_{\phi_3}(\zeta_{\phi_2}) \tag{35}$$

Now, define ζ_{ϕ_2} as

$$\zeta_{\phi_2} \equiv \nu_2 + \sigma_{\phi_4}(\zeta_{\phi_3}) \tag{36}$$

Let us rewrite (35) as

$$\dot{\nu}_2 = -\sigma_{\phi_3}(\nu_2 + \sigma_{\phi_4}(\zeta_{\phi_3})) \tag{37}$$

We chose

$$M_{\phi_3} \geq 2M_{\phi_4} \tag{38}$$

We then have that in a finite time, $\exists T_3$ such that $\mid \nu_2 \mid \leq M_{\phi_4}$ for $t \geq T_3$, this implies from (33) that $\dot{y}$ is bounded.

For $t \geq T_3$, $\mid \nu_2 + \sigma_{\phi_4}(\zeta_{\phi_3}) \mid \leq 2M_{\phi_4}$. It then follows that, $\forall t \geq T_3$

$$\sigma_{\phi_3}(\nu_2 + \sigma_{\phi_4}(\zeta_{\phi_3})) = \nu_2 + \sigma_{\phi_4}(\zeta_{\phi_3}) \tag{39}$$

Thus, after time T_3, (37) reduces to

$$\dot{\nu}_2 = -\nu_2 - \sigma_{\phi_4}(\zeta_{\phi_3}) \tag{40}$$

4) Boundedness of y: To establish a bound for y, let us define

$$\nu_3 \equiv \nu_2 + 2\frac{\dot{y}}{g} + \phi + \frac{y}{g} \tag{41}$$

then

$$\dot{\nu}_3 = \dot{\nu}_2 + 2\frac{\ddot{y}}{g} + \dot{\phi} + \frac{\dot{y}}{g} \tag{42}$$

Finally using (16), (32), (37) and (39) into (42), we obtain

$$\dot{\nu}_3 = -\sigma_{\phi_4}(\zeta_{\phi_3}) \tag{43}$$

We propose ζ_{ϕ_3} of the following form

$$\zeta_{\phi_3} \equiv \nu_3 \tag{44}$$

then

$$\dot{\nu}_3 = -\sigma_{\phi_4}(\nu_3) \tag{45}$$

5) Convergence of $\phi, \dot{\phi}, \dot{y}$ and y to zero: From (45) it follows that for a time large enough $\nu_3 \rightarrow 0$. From (37) it follows that $\nu_2 \rightarrow 0$ and from equation (36) $\zeta_{\phi_2} \rightarrow 0$. From (30) $\nu_1 \rightarrow 0$ then from (29) $\zeta_{\phi_1} \rightarrow 0$.

We can see from equation (21) that $\dot{\phi} \rightarrow 0$. From equation (22) we get $\phi \rightarrow 0$. From (33) $\dot{y} \rightarrow 0$ and finally from (41) $y \rightarrow 0$.

The control input $\tilde{\tau}_\phi$ is given by

$$\begin{aligned} \tilde{\tau}_\phi \;=\; & -\sigma_{\phi_1}(\dot{\phi} + \sigma_{\phi_2}(\phi + \dot{\phi} + \\ & \sigma_{\phi_3}(2\phi + \dot{\phi} + \frac{\dot{y}}{g} + \\ & \sigma_{\phi_4}(\dot{\phi} + 3\phi + 3\frac{\dot{y}}{g} + \frac{y}{g})))) \end{aligned} \tag{46}$$

C. Control of the pitch angle and the horizontal displacement in the x -axis

From equations (17) and (18) we obtain $\phi \rightarrow 0$, then from (12) gives

$$\ddot{x} = -g\tan\theta \tag{47}$$

Finally we take the sub-system

$$\ddot{x} \;=\; -g\tan\theta \tag{48}$$

$$\ddot{\theta} \;=\; \tilde{\tau}_\theta \tag{49}$$

As before, we assume that the control strategy will insure a very small bound on $\mid \theta \mid$ in such a way that $\tan(\theta) \approx \theta$. Therefore (48) reduces to

$$\ddot{x} = -g\theta \tag{50}$$

Using a procedure similar to the one proposed for the roll control we obtain

$$\begin{aligned} \tilde{\tau}_\theta \;=\; & -\sigma_{\theta_1}(\dot{\theta} + \sigma_{\theta_2}(\theta + \dot{\theta} + \\ & \sigma_{\theta_3}(2\theta + \dot{\theta} - \frac{\dot{x}}{g} + \\ & \sigma_{\theta_4}(\dot{\theta} + 3\theta - 3\frac{\dot{x}}{g} - \frac{x}{g})))) \end{aligned} \tag{51}$$

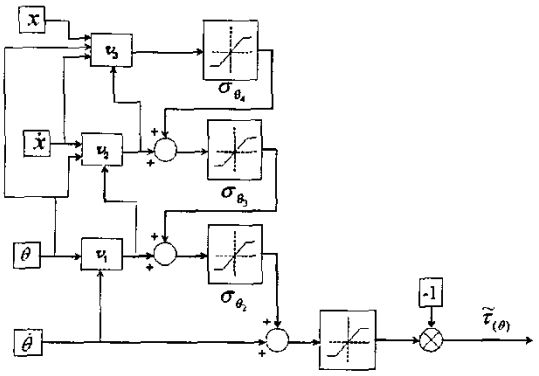

Fig. 6. Pitch control scheme.

IV. Experimental results

The control algorithm proposed above has been tested in real-time experiments. The experimental platform is composed of a Draganfly four-rotor rotorcraft, a Futaba 72 MHz radio, a PC pentium II and a 3D tracker system (POLHEMUS) [3] for measuring the position (x, y, z) and orientation (ψ, θ, ϕ) of the rotorcraft. The Polhemus is connected via RS232 to the PC (see Fig. 7).

The radio and the PC (INTEL Pentium II) are connected using data acquisition cards (ADVANTECH PCL-818HG and PCL-726).

In order to simplify the experiments, the control inputs can be independently commuted between the automatic and the manual control modes (see Fig. 7).

The connection in the radio is directly made to the joystick potentiometers for the gas, yaw, pitch and roll controls. The rotorcraft evolves freely in a 3D space without any flying stand. The control law also requires the time derivatives of the position (x, y, z) and the orientation (ψ, θ, ϕ).

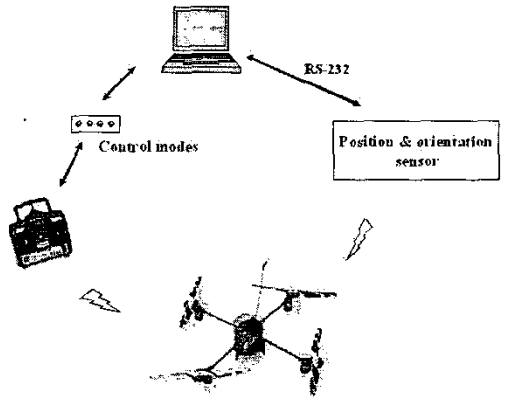

Fig. 7. Real-Time architecture of the platform.

Phase	*Control parameter*	*Value*
1	a_{z_1}	0.001
	a_{z_2}	0.002
2	a_{ψ_1}	2.374
	a_{ψ_2}	0.08
3	M_{ϕ_1}	2
	M_{ϕ_2}	1
	M_{ϕ_3}	0.2
	M_{ϕ_4}	0.1
4	M_{θ_1}	2
	M_{θ_2}	1
	M_{θ_3}	0.2
	M_{θ_4}	0.1
1 – 4	T	$\frac{1}{14}s$

TABLE II

GAIN VALUES USED IN THE CONTROL LAW

They are obtained in practice using the following approximation $\dot{q}_t \approx \frac{q_t - q_{t-T}}{T}$, where q is a given variable and T is the sampling period. The controller parameters that were used in the experiment are given in Table II. These parameters were tuned to obtain the best performance in practice

The control objective in the practical experiment was to make the mini-rotorcraft hover at an altitude of 30 [cm], i.e. we wish to reach the position $(x, y, z) = (0, 0, 30\ [cm])$ while $(\psi, \theta, \phi) = (0, 0, 0)$ (see Fig. 8).

Figures 8 and 9 show the performance of the controller when applied to the rotorcraft.

V. CONCLUSION

We have proposed a stabilization control algorithm for a mini-rotorcraft having four rotors. The dynamic model of the rotorcraft was obtained via a Lagrange approach and the proposed control algorithm is based on Lyapunov analysis.

The proposed strategy has been successfully applied to the mini-rotorcraft, and the experimental results have shown that the controller performs satisfactorily. We have done some videos of the experiments.

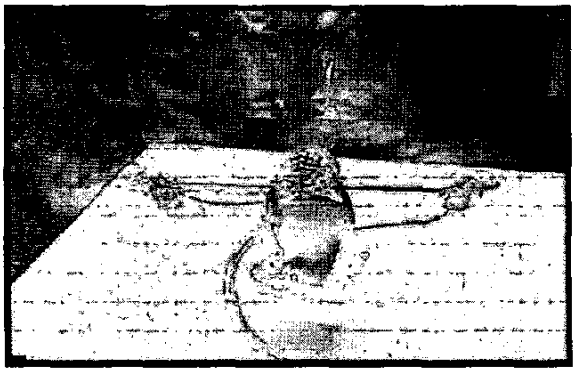

Fig. 8. Real-time control of the rotocraft.

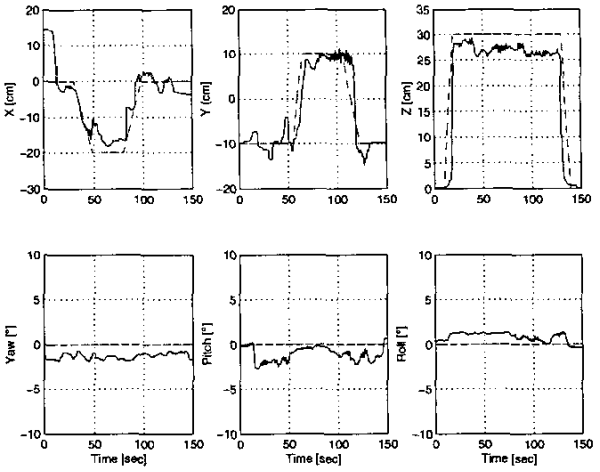

Fig. 9. Position and orientation of the rotorcraft. The dotted lines represent the desired trajectory

REFERENCES

[1] Barnes W. McCormick, *Aerodynamics Aeronautics and Flight Mechanics*, John Wiley & Sons, INC., New York, 1995.

[2] Hauser J., Sastry S. & Meyer G., Nonlinear control design for slightly nonminimum phase systems: Application to V/STOL aircraft, *Automatica*, 28(4):665-679, 1992.

[3] Fastrack 3Space Polhemus, *User's Manual*, Colchester, Vermont, USA.

[4] Lozano R., Brogliato B., Egeland O., Maschke B. *Passivity-based control system analysis and design*. Springer-Verlag, Communications and Control Engineering Series, 2000. ISBN 1-85233-285-9.

[5] Fantoni I., Lozano R., *Control of nonlinear mechanical underactuated systems*. Springer-Verlag, Communications and Control Engineering Series, 2001.

[6] Marconi L., Isidori A., Serrani A., Autonomous vertical landig on an oscillating platform: an internal-model based approach, *Automatica*, 38: 21-32, 2002.

[7] Wayner P., Gyroscopes that don't spin make it easy to hover. New York Times, 8th of August 2002.

[8] Alderete T. S., Simulator aero model implementation, NASA Ames Research Center, Moffett Field, California.

[9] Etkin B., *Dynamics of Flight*, John Wiley and Sons, Inc., New York, 1959.

[10] Goldstein H., *Classical Mechanics*, Second Edition, Addison Wesley, 1980.